Neutron Detection Using Shards Of ^{6}Li Glass Scintillator

Steven J. Gardiner

A senior thesis submitted to the faculty of
Brigham Young University
in partial fulfillment of the requirements for the degree of

Bachelor of Science

Lawrence B. Rees, Advisor

Department of Physics and Astronomy

Brigham Young University

August 2012

ABSTRACT

Neutron Detection Using Shards Of ^{6}Li Glass Scintillator

Steven J. Gardiner
Department of Physics and Astronomy
Bachelor of Science

Due to a worldwide shortage of ^{3}He, a key component of many neutron detectors, alternative technologies are needed to fully secure the world against the threat of nuclear terrorism. Lithium-6-loaded glass scintillator is a material that has been widely used in neutron detectors for decades, but its comparatively high gamma sensitivity has made it unattractive for use in homeland security applications. We have recently identified and tested a new method for reducing the gamma sensitivity of a neutron detector constructed using ^{6}Li-loaded glass scintillator. Our prototype neutron detector consists of small (1 mm^3) shards of broken ^{6}Li-loaded glass scintillator embedded in a matrix of Eljen Technology EJ-500 optical epoxy. Several inches of mineral oil can be placed behind the matrix for moderation. Monte Carlo simulations (conducted using the particle transport codes MCNP and PENELOPE) and experimental tests both show that this detector can achieve good neutron detection efficiency while obtaining dramatically reduced gamma sensitivity when it is compared to similar detectors that employ sheets of ^{6}Li glass.

ACKNOWLEDGMENTS

I am sincerely grateful to Dr. Lawrence Rees and Dr. J. Bart Czirr for the many hours they spent teaching me and helping me grow as a young physicist. I also wish to thank my wife Lindsey for her careful editing and loving support.

Contents

Chapter 1

Introduction

1.1 Motivation

Ever since the horrific events of September 11, 2001, the US government has made preventing another terrorist attack on American soil a top priority. Although future terrorist attacks could come in a variety of forms, none of the possible scenarios is more nightmarish than the detonation of a nuclear weapon in a large city. Even if the terrorist enemies of the United States were unable to construct a fully functional atomic bomb, they could still use a radiological dispersal device (e.g., a conventional explosive laced with radioactive materials) to take lives and contaminate neighborhoods. [1]

1.1.1 Countering the Threat of Nuclear Terrorism

In order to protect the nation from a possible nuclear attack, the Department of Homeland Security (DHS) has placed radiation portal monitor systems at US ports of entry to detect illicit nuclear materials. [2] These radiation portal monitors (RPMs) detect the presence of gamma rays and neutrons, both of which are forms of radiation produced by key components of nuclear weapons such

as uranium and plutonium. Through the National Nuclear Security Administration's (NNSA) Second Line of Defense program, radiation portal monitors are also being installed in various locations around the world. [3–5] The security of many nations depends on the ability of these systems to reliably discern the presence of hidden nuclear material in vehicles, in shipping containers, and on people.

Radiation portal monitors generally use separate gamma ray and neutron detection systems in order to maximize the probability of detecting a smuggled nuclear weapon. Because gamma rays are produced by all radioactive materials that are potential security threats, gamma ray detectors serve as the primary component of RPMs. These detectors use well-understood technology, are relatively cheap to manufacture, and are commercially available from a number of vendors. [6]

Although gamma ray detectors are the principal means of identifying concealed radioactive sources using RPMs, separate neutron detectors are usually also included in these systems. Neutron detectors complement gamma ray detectors in RPMs because some potentially dangerous nuclear materials (especially the atomic bomb ingredient plutonium) emit significant levels of neutron radiation. Because RPMs are becoming increasingly common at ports of entry around the world, terrorists attempting to transport a nuclear weapon would be likely to conceal it using a shield of material that absorbs radiation. However, since the materials that absorb gamma rays well (heavy elements) and the materials that absorb neutrons well (light elements) are different, constructing a shield that would absorb both kinds of radiation and be small enough to go unnoticed by security personnel would likely be very difficult. [7] Including neutron detectors in an RPM therefore offers the possibility of detecting certain nuclear materials that have been hidden from gamma ray detectors.

1.1.2   The ^{3}He Crisis

One major obstacle to the widespread use of neutron detectors in RPMs has been a global short-age of helium-3 (^{3}He), an extremely rare isotope of helium. Neutron detectors constructed using metal tubes filled with pressurized ^{3}He have historically been the preferred choice for radiation portal monitors due to their high detection efficiency, durability, and low sensitivity to gamma radiation. [8] Although ^{3}He can be extracted in trace amounts from any natural source of helium gas, [9] the only currently available means of obtaining ^{3}He in significant quantities is to harvest it from decaying tritium found in aging nuclear weapons.[1] [10] As a result of post-Cold-War nuclear disarmament, the US has not manufactured tritium in significant quantities since 1988. [9] Due to the resulting decrease in the amount of available tritium (and, therefore, ^{3}He) and a sharp increase in the demand for ^{3}He for homeland security applications in recent years, the entire world supply of ^{3}He is insufficient to meet current needs. [10]

In an effort to work around the ^{3}He supply problem, the US government is currently funding many research and development projects aimed at replacing the standard ^{3}He-based RPM neutron detectors with alternative models that utilize more easily available materials. Although several mature neutron detector designs exist which do not use ^{3}He, [11–14] and many more are in various stages of development, [8, 15, 16] constructing a replacement neutron detector which matches or exceeds the performance of comparable ^{3}He-based models in every way is a difficult task.

1.2   Performance Criteria for RPM Neutron Detectors

In order to ensure that candidate ^{3}He-replacement neutron detectors will perform at least as well as the old technology, the DHS has established strict requirements that must be met before any

---

[1]With a half-life of 12.3 years, tritium undergoes beta-minus decay to become helium-3 via the reaction

$$^3_1\text{H} \rightarrow {}^3_2\text{He} + \beta^- + \bar{\nu}_e + 18.6 \text{ keV}.$$
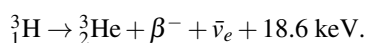
replacement will be seriously considered. [17] Although many of these requirements involve tests that must be performed with a detector that is ready for installation (e.g., tests of the detector's environmental hardiness and operational lifetime), three of the performance criteria are particularly important for prototype detectors: absolute detection efficiency, gamma sensitivity, and the gamma absolute rejection ratio for neutrons (GARRn). [18]

1.2.1   Neutron Detection Efficiency

The absolute neutron detection efficiency of a detector is defined as the fraction of neutrons emitted by a source that are detected. Because the measured absolute efficiency of a neutron detector depends on the details of the experimental setup (e.g., the distance from the source to the detector, the orientation of the detector, etc.), one must specify the geometry of the testing situation in order for an absolute efficiency value to have any meaning. To avoid this strong dependence on testing geometry, scientists will sometimes report the efficiency of a neutron detector in terms of its intrinsic efficiency, which is defined as the fraction of neutrons striking the detector that are detected. [19] Since the specific neutron emission rate (i.e., the number of neutrons emitted per second per unit mass of a material) of californium-252 (^{252}Cf, a neutron source that is commonly used in research) is well-known,[2] absolute efficiency measurements are also often reported in units of counts per second per nanogram of ^{252}Cf (cps/ng ^{252}Cf) present in the source. The fraction of emitted neutrons that are detected can be recovered from this figure by dividing it by the specific neutron emission rate of ^{252}Cf.

The requirements published by the DHS specify that any acceptable ^{3}He-replacement neutron detector must have an absolute neutron detection efficiency of at least $2.5\,\mathrm{cps/ng}\ ^{252}$Cf (about 10^{-3} detected neutrons per emitted neutron) when a ^{252}Cf source is placed 2 m away from the center of the front face of the detector. [17] Researchers at Pacific Northwest National Laboratory (PNNL)

---

[2]The specific neutron emission rate of ^{252}Cf is 2.314×10^3 neutrons per second per nanogram. [20]

recommend that this test be performed with the [252]Cf source surrounded by 0.5 cm of lead and 2.5 cm of polyethylene to simulate a concealed neutron source. [18]

1.2.2 Gamma Sensitivity

The gamma sensitivity of a neutron detector is defined as the fraction of gamma rays striking the detector that are misidentified as neutrons by the detector. [18] Although most neutron detectors are designed to ignore other forms of radiation as much as possible, a wide variety of neutron detectors (including [3]He-based detectors) will occasionally be "fooled" by a gamma ray that interacts with the detector in a way that makes it appear to be a neutron. While some gamma sensitivity is not a problem for neutron detectors in many appplications, neutron detectors in RPMs that are more than minimally gamma sensitive can lead to high operational costs. Since legitimate sources of neutrons are rare and the level of ambient neutron radiation from the environment (e.g., cosmic ray neutrons) is generally quite low, any RPM neutron detector alarms must be treated very seriously by security personnel as a possible threat. Neutron detectors that misfire often could therefore result in frequent and lengthy searches for non-existent sources of neutron radiation. These false alarms would undoubtedly frustrate security officers and private citizens, impede the flow of trafffic, and erode public confidence in homeland security RPM systems. Because innocuous gamma ray sources are fairly common[3] and the normal level of environmental gamma radiation is many times higher than that of neutron radiation, neutron detectors that respond to gamma rays at a significant rate are unacceptable for use in RPMs. [8] In order to prevent false neutron detector alarms as much as possible, the DHS has mandated that any acceptable [3]He-replacement neutron detector must have a gamma sensitivity of 10^{-6} or less. [17, 18]

---

[3]Some common sources of gamma rays in shipping containers include kitty litter, tile, and fertilizer. [6, 21] People that have recently been diagnosed or treated using radiopharmaceuticals also emit enough gamma radiation to be a common cause of RPM gamma ray detector alarms. [22]

1.2.3   Gamma Absolute Rejection Ratio for Neutrons (GARRn)

The gamma absolute rejection ratio for neutrons (GARRn) of a neutron detector is defined as

$$GARRn \equiv \frac{\varepsilon_{abs,n+\gamma}}{\varepsilon_{abs,n}}$$

where $\varepsilon_{abs,n+\gamma}$ is the measured absolute efficiency of the detector with both a neutron source and a strong[4] gamma ray source present and $\varepsilon_{abs,n}$ is the measured absolute efficiency with only the neutron source present. The neutron source should be configured in both cases as it would be for the absolute efficiency measurement mentioned above. [18] This characteristic of a neutron detector is a quantitative measure of how much a strong gamma ray source interferes with the detector's ability to detect a neutron source. Because a terrorist group could conceivably hide dangerous nuclear material inside of a large container filled with ordinary material that is slightly radioactive (e.g., kitty litter) or in a shipment of legitimate radiopharmaceuticals, RPM neutron detectors must perform well even while exposed to high levels of gamma radiation. [6] To ensure that RPM neutron detectors will perform well under such conditions, the DHS requires a measured GARRn between 0.9 and 1.1 for any neutron detector to be acceptable. [17, 18]

1.3 ^{6}Li Glass Scintillator as an Alternative to ^{3}He

One mature alternative technology for detecting neutrons is cerium(III)-activated lithium-6-loaded glass scintillator. Since its development in the late 1950s, this material has been commonly used to detect neutrons and other forms of radiation in a variety of scientific and industrial contexts. [23]

---

[4]The gamma ray source for GARRn measurements should uniformly irradiate the front face of the detector with an exposure rate of at least 10 mR/h (about 4500 $\gamma/\text{cm}^2 \cdot$ s for a cobalt-60 source). [18]

1.3.1   Neutron Detection Mechanism

Scintillators are materials which fluoresce when stimulated by ionizing radiation. Lithium-6-loaded glass scintillator exploits the lithium-6 (^{6}Li) neutron capture reaction,

$$^6_3\text{Li} + {}^1_0\text{n} \rightarrow {}^7_3\text{Li}^* \rightarrow {}^4_2\alpha + {}^3_1\text{T} + 4.78 \text{ MeV}$$
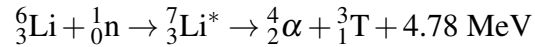
to produce energetic charged particles (an alpha particle and a triton) which subsequently collide with nearby atoms in the glass and eject some of their electrons. The ejected electrons then migrate through the glass and undergo many collisions with surrounding particles. Some of these migrating electrons will transfer energy to the outer electrons of cerium(III) (Ce^{3+}) ions in the glass, causing them to enter an excited state. After about 0.14 μs, the excited electrons will relax back into their original state, usually by emitting a photon with a wavelength of around 395 nm to carry off the excess energy. [24] Because the charged products of a neutron capture reaction in the glass can cause the emission of many such photons in a short period of time, a pulse of UVA light is emitted by the glass. This light can be detected by appropriate equipment (e.g., a photomultiplier tube) and converted into an electrical signal. A more detailed description of the light production mechanism in ^{6}Li-loaded glass scintillator can be found in appendix B.

1.3.2   The Gamma Sensitivity Problem

Although ^{6}Li-loaded glass scintillator is highly responsive to slow neutrons, it misidentifies gamma rays as neutrons much more often than ^{3}He, which makes it less attractive than ^{3}He for applications (such as RPMs) in which the ability to make independent but simultaneous checks for the presence of gamma rays and neutrons is important. [8] Lithium-6-loaded glass scintillator is sensitive to gamma rays because a gamma ray passing through the glass will sometimes strike an electron and transfer enough energy to the electron to eject it from its host atom. The ejected electron will then travel through the glass and remove additional electrons from atoms nearby. These electrons can

remove even more neighboring electrons from their atomic orbitals, and the process will continue as a chain reaction until the electrons no longer have enough energy to ionize additional atoms. As the liberated electrons travel through the glass, some of them will excite the outer electrons of Ce^{3+} ions, causing them to emit the same photons that are produced as the result of a neutron capture reaction. For neutron detectors based on ^{6}Li-loaded glass scintillator to function properly in the presence of gamma radiation, the detectors must therefore either discriminate between light pulses generated by neutrons and gamma rays or limit the number of incident gamma rays that generate a significant amount of scintillation light.

1.3.3 Solutions Based on Pulse Discrimination

One way of reducing the gamma sensitivity of ^{6}Li-loaded glass scintillator is to discriminate between light pulses generated by neutrons and gamma rays. Three techniques are generally used to distinguish between these two kinds of pulses: pulse height discrimination, pulse shape discrimination, and anticoincidence counting.

1.3.3.1 Pulse Height Discrimination

Pulse height discrimination distinguishes between light pulses generated by neutrons and gamma rays based on their brightness. Although both neutrons and gamma rays entering ^{6}Li glass can induce scintillation, gamma rays that scatter in the glass generally cause the production of fewer photons (and therefore dimmer light pulses) than neutrons captured by ^{6}Li nuclei. A photodetector responding to these light pulses will register voltage spikes whose size (measured using either height or total area) is roughly proportional to the total number of photons produced.[5] Therefore,

---

[5]The response of a photodetector can vary between pulses of equal brightness. Some factors that influence the response include where the light is produced, how much of it is successfully collected by the photodetector, and statistical variations in the behavior of each of the photodetector components. On average, however, the voltage spikes

if a neutron detector operator configures the system to ignore voltage spikes in the photodetector that are lower than an appropriate threshold, most of the gamma-ray-induced scintillation events will be eliminated without significantly reducing the number of neutron events. Pulse height discrimination of this kind is widely used in a variety of neutron detectors, including ^{6}Li glass-based neutron detectors.

1.3.3.2 Pulse Shape Discrimination

Pulse shape discrimination distinguishes between neutrons and gamma rays by looking for differences in the way that the brightness of the scintillation light induced by each kind of particle varies over time. Such differences will be reflected in the shape of the electrical pulses created by a photodetector monitoring the scintillator. [19] If a neutron detector is configured to reject pulses that have a shape associated with gamma ray interactions, then its gamma ray sensitivity can be significantly reduced.

1.3.3.3 Anticoincidence Counting

Anticoincidence counting relies on a signal from a secondary particle detector to determine whether a pulse from the primary neutron detector should be accepted or rejected. For neutron detectors based on ^{6}Li-loaded glass scintillator, the secondary detector is usually designed to detect energetic electrons that are scattered out of the glass by gamma rays. If a pulse from the neutron detector is received approximately simultaneously with a signal from the secondary detector, the neutron detector pulse will be rejected as originating from a gamma ray interacting in the glass scintillator.

produced in the photodetector in response to incoming light will be proportional to the number of photons produced by the light source.

1.3.3.4   Review of Previous Work

The possibility of using pulse shape discrimination techniques to reduce the gamma sensitivity of neutron detectors based on ^{6}Li glass scintillator has been investigated in a number of experiments. [25–27] Unfortunately, these experiments demonstrated that the differences in the light pulses produced by various compositions of ^{6}Li glass in response to neutrons and gamma rays are too small to be useful for significant pulse shape discrimination. As a result, pulse shape discrimination has only ever led to meager reductions in the gamma sensitvity of neutron detectors that use ^{6}Li glass as their only scintillating material.

Recent work at Brigham Young University has demonstrated that adding an auxiliary plastic scintillator (for the detection of electrons scattered by gamma rays) to a neutron detector based on ^{6}Li-loaded glass scintillator can enable effective pulse shape discrimination. [28] When a thin sheet of ^{6}Li-loaded glass scintillator is placed on top of a slab of plastic scintillator, many of the electrons scattered by gamma rays in the glass will leak out of the glass into the plastic scintillator. Because the glass and plastic scintillators are both optically coupled to the same photodetector, these electrons will create scintillation pulses with one component that originates in the glass and another component that originates in the plastic. Since the charged products of a neutron capture reaction in the glass have a comparatively short range, very few scintillation pulses generated by neutrons will have a significant plastic component. A pulse can be checked for a significant plastic component by integrating the pulse over time to find its total area and its "early" area (the area obtained by integrating between the beginning of the pulse and a certain elapsed time). Because the plastic produces the majority of its scintillation light over a shorter time period than the glass, pulses that have a significant plastic component will have a disproportionately large early area. By configuring this neutron detector so that all pulses that have a total area less than a certain threshold (pulse height discrimination) and all pulses that have a ratio of early area to total area above a certain threshold (pulse shape discrimination) are rejected, researchers at BYU have shown

that the fraction of incident gamma rays that are misidentified as neutrons can be lowered to about 10^{-4} while maintaining good neutron detection efficiency. [28]

The possible use of anticoincidence counting to reduce the gamma sensitivity of neutron detectors based on ^{6}Li-loaded glass scintillator has been considered since at least 1961. [29] Measurements performed several decades ago by Jensen and Czirr assessed the usefulness of an anticoincidence method for a neutron detector constructed using a thin disk of ^{6}Li glass placed inside of a plexiglass light pipe and sandwiched between two slabs of plastic scintillator. [30] Highly reflective aluminum foil was used to optically isolate the two kinds of scintillator from each other, and separate photodetectors were used to simultaneously measure the light output of the two independent systems. Several thicknesses of glass scintillator were tested with several incident gamma ray energies. In every case, these researchers found that a large fraction (results varied between 49 and 85% depending on the configuration) of the gamma-ray-induced light pulses in the detector that were intense enough to be mistaken for neutrons occurred simultaneously with light pulses in the plastic scintillator. These simultaneous plastic scintillator pulses were attributed to electrons that were scattered by gamma rays in the glass and then leaked out into the plastic. Unfortunately, this anticoincidence method was found to be impractical due to problems associated with poor optical coupling between the glass disk and the light pipe. More recently, however, a variation of this anticoincidence method has been applied with some success to detectors based on thin fibers of ^{6}Li glass. [31, 32]

1.3.4 Solutions Based on Reducing Gamma-Induced Scintillation

Another method of reducing the gamma sensitivity of ^{6}Li glass is to limit the number of incident gamma rays that induce significant scintillation.

1.3.4.1 Thin Sheet Method

One way of doing this takes advantage of the range difference between the charged products of a ^{6}Li neutron capture reaction (an alpha particle and a triton) and electrons traveling through the glass. In any standard ^{6}Li glass scintillator, the maximum ranges of an alpha particle and a triton are about 7 μm and 40 μm,[6] respectively, while the maximum range of an electron scattered by a gamma ray is often as large as 1 mm or more. [19, 24] Therefore, if a thin sheet (~1 mm thick) of ^{6}Li glass is used to detect neutrons, most of the high-energy electrons will leak out and very few of the neutron capture products will do so. Because most of the high-energy electrons will escape from the glass before depositing their full energy, few incident gamma rays will be able to trigger intense scintillation pulses. Although a fair number of gamma rays will still trigger the production of a comparatively small amount of light, these events can be easily ignored using pulse height discrimination. A number of experiments have confirmed that the gamma sensitivity of ^{6}Li glass scintillator decreases substantially as the glass is made progressively thinner. [29, 30, 33] However, reducing the thickness of a sheet of ^{6}Li glass in a neutron detector also reduces its neutron detection efficiency, both because less glass is available for capturing neutrons and because, for very thin sheets of glass, a signficant fraction of the neutron capture products can leak out.

1.3.4.2 Fiber Method

An interesting variation on this method for reducing the gamma sensitivity of ^{6}Li-loaded glass scintillator, developed at PNNL and licensed to Nucsafe, LLC, for use in commercial neutron detectors, employs thin (~0.1 mm diameter) fibers of scintillating glass. [8, 13] These fibers may be coated with or embedded in a suitable polymer to increase their durability and to slow down incident neutrons, increasing the likelihood that the neutrons will be detected. [34]

---

[6]Although the alpha particle and triton also scatter electrons in the glass, since the maximum ranges for electrons scattered by these particles are 0.0196 μm (α) and 0.0648 μm (T), they may be safely ignored for our purposes. [24]

1.3.4.3   Small Ball Method

Another proposed variation on the glass sheet technique is based on the observation that, occasionally, an electron scattered in a thin sheet of ^{6}Li glass will travel primarily in the plane of the glass and deposit all or most of its energy therein. Such an electron will generate a pulse of scintillation light that will be too intense to be distinguished from a neutron-induced pulse via pulse height discrimination. Soon after the invention of ^{6}Li glass scintillator, researchers at Argonne National Laboratory perceived this problem and put forward a method for solving it. At an international symposium on neutron physics in 1961, L. M. Bollinger made the following remark:

> We are attempting to make a detector that is very insensitive to γ-rays by using small balls of either a B- or a Li-glass scintillator. The scintillating balls are embedded in a transparent medium that does not scintillate. It is hoped that, because of the difference in the ranges of the electrons and the reaction products, we will be able to find a ball size for which the medium will be sensitive to neutrons, but insensitive to γ-rays. It is also hoped that, by a proper adjustment of the refractive indices, it will be possible to extract most of the light . . . . The work at Argonne is being done by Dr. [G. E.] Thomas. [29]

By using these small balls of ^{6}Li glass scintillator rather than a thin sheet, researchers at Argonne National Laboratory eliminated the plane of the glass. This would presumably increase the number of scattered electrons that would leak out of the glass, reducing the glass's gamma sensitivity. Despite this statement in a public forum, to the best of my knowledge, no formal report describing the results of this research or even describing this technique in more detail was ever published. Leaving this technique untested neglects a possibly valuable method for reducing the gamma sensitivity of ^{6}Li glass scintillator to a level low enough for use in radiation portal monitors.

1.3.5   A New Proposed Solution

In this thesis, I will present and evaluate a modified version of the gamma sensitivity reduction technique just mentioned. A neutron detector constructed using the technique I will present, often referred to hereafter as the "broken glass detector," consists of small (~1 mm^3) shards of ^{6}Li-loaded glass scintillator distributed within a matrix made of a hydrogenous, UVA-transparent material that is optically coupled to a photomultiplier tube. The signal from the photomultiplier tube is digitized, and both pulse height and pulse shape discrimination are applied to eliminate background noise from the neutron detector signal.

I will show that a neutron detector constructed using this method can achieve a gamma sensitivity low enough to satisfy the DHS RPM requirement without sacrificing high neutron detection efficiency. The dramatic reduction in gamma sensitivity available through this method gives me hope that an array of these broken glass detectors may be able to satisfy all of the DHS RPM criteria. Such a large-scale detector could potentially serve as a viable alternative to ^{3}He-based neutron detectors and offer the world additional protection against the threat of nuclear terrorism.

Chapter 2

Monte Carlo Simulations

The Monte Carlo method is a technique for modeling interactions of particles with matter. Rather than explicitly solving a complex differential equation to determine the average behavior of particles emitted from a radiation source, a Monte Carlo simulation uses random numbers and probabilities tabulated from experimental data to simulate the trajectory and interactions (collectively referred to as a "history") of a particle emerging from a source in a specified geometry. As a particle history is being simulated, quantities of interest are monitored by tallies, and the tally scores are modified by the particle whenever it behaves in relevant ways. If a program repeatedly generates and tracks particles through a region of interest until a sufficiently large number of particle histories have been simulated, the average behavior of the particles can be determined using the tally results and the central limit theorem. [35]

2.1   Simulation Methods

I used Monte Carlo simulations to shed light on the physical processes at work within the broken glass detector and inform the design of prototypes for experimental testing.

2.1.1 Particle Transport Codes

To conduct Monte Carlo simulations of the broken glass detector, I used two particle transport code packages: (1) MCNP5 (Monte Carlo N-Particle, version 5), developed by many people at Los Alamos National Laboratory, and (2) PENELOPE-2008 (PENetration and ENergy LOss of Positrons and Electrons, 2008 version), produced by Francesc Salvat, José M. Fernández-Varea, and Josep Sempau of the University of Barcelona. I used MCNP as a general-purpose package to calculate simulated values for the neutron detection efficiency and gamma sensitivity of a variety of broken glass detector configurations. Although PENELOPE cannot simulate neutron transport, I found it helpful to compare its calculated gamma sensitivity results to the output of MCNP as a validity check.[1] I also preferred to use PENELOPE to calculate theoretical gamma sensitivity values whenever possible[2] because it was generally three times faster than MCNP for comparable problems.

2.1.2 Automated Input File Generation Using Mathematica

The most difficult part of preparing Monte Carlo simulations is usually specifying the geometry of the source and objects through which the simulated particles will travel. Both MCNP and PENELOPE represent space as a collection of regions bounded by quadric surfaces.[3] Each region

---

[1]PENELOPE handles some aspects of coupled photon-electron transport in more detail than MCNP. For example, MCNP5 ends electron histories whenever the electron energy falls below 1 keV (or a higher, user-defined cutoff energy) and assumes that all of the remaining electron energy is deposited in its final location. PENELOPE allows this cutoff energy to be as low as 50 eV. [36] Despite the additional approximations used in MCNP, however, the results of energy deposition and gamma sensitivity calculations performed in this study using both codes agreed quite well.

[2]PENELOPE performs comparatively rapid photon transport simulations, but its default capacity for complex geometry (a maximum of 9,999 surfaces) is very limited compared to that of MCNP (a maximum of 99,999 unique surfaces plus repeated structure capabilities).

[3]Quadric surfaces are sets of points in 3D space which may be represented by the equation $A_{xx}x^2 + A_{xy}xy + A_{xz}xz + A_{yy}y^2 + A_{yz}yz + A_{zz}z^2 + A_xx + A_yy + A_zz + A_0 = 0$, where the A_i are real constants. [36]

may be assigned a material composition (typically specified using elemental ratios) and a density. While this approach to representing geometrical relationships can be computationally efficient, writing a correct input file for either of these codes rapidly becomes difficult as the number of surfaces needed to specify the geometry of a problem grows.

Simulating a broken glass detector using MCNP or PENELOPE is especially difficult due to the complicated geometry that must be represented. For a broken glass detector that contains the equivalent of a 1 mm-thick circular sheet of glass that is 5 inches in diameter (a standard size commonly used with photomultiplier tubes), 12,668 shards with a volume of 1 mm^3 each must be dispersed within a transparent medium. While MCNP offers repeated structure features that make specifying a regular lattice of many objects very simple, asymmetries such as irregular glass shard placement, irregular spacing between shards, and arbitrary orientations for asymmetrical shards could be quite difficult to specify and even more difficult to debug while using a lattice geometry. Since all surfaces must be explicitly specified in a PENELOPE input file, using a lattice geometry in MCNP was also undesirable because this would make translating simulation instructions between the two codes particularly difficult.

To enable myself to rapidly produce MCNP and PENELOPE input files specifying the geometry and Monte Carlo simulation parameters for a variety of broken glass detectors under a variety of conditions, I developed a package of Wolfram Mathematica functions to automatically generate these files based on simple user input. In all cases, the region of interest is described as a sphere containing a cylindrical detector and a point radiation source located at some arbitrary distance perpendicular to the center of the front face of the detector. The detector, typically described as being made of either PMMA[4] or polyvinyl toluene (this material and all others, however, are fully customizable), contains a user-defined number of either spherical or spheroidal bodies that rep-

---

[4]Poly(methyl methacrylate) is a transparent polymer often sold under the trade names Plexiglas, Perspex, and Lucite.

resent shards of [6]Li glass. The dimensions of the glass shards are specified by the user, and the user can exert a high degree of control over how they are distributed within the volume of the detector. Although all the shards are currently generated by the program with identical dimensions, the code could be modified fairly easily to allow them to each be uniquely generated with dimensions distributed according to a user-defined scheme. The input file generation program also draws one or two spherical surfaces around the point source that may be used to define up to two layers of shielding with arbitrary thickness and composition. Similarly, the user can add a cylinder of arbitrary thickness and composition in front of and behind the detector.

The Mathematica code can render three-dimensional views of the large-scale geometry and the layout of the glass shards. For MCNP input files, it also generates a header describing the detector in detail (including the total mass and volume of the glass shards, the solid angle[5] subtended by the detector at the point source, etc.). For speed, the code can automatically bias the source to only generate particles that will hit the detector while modifying the statistical weight of the particles so that all tally results will be computed as if the source were isotropic. In addition to input file generation tools, the package includes a number of functions for parsing, analyzing, and displaying information about the simulation results, as well as a tool for calculating the solid angle subtended by a right circular cylinder at an arbitrary point.[6]

Interested readers can obtain a copy of the latest version of this Mathematica package (which, as of this writing, is compatible with Mathematica 7 or higher) by contacting me directly at gardiner.steven@gmail.com. For more information about the features available in this Mathematica

---

[5]The solid angle subtended by a smooth parametric surface at a given point is defined as the set of lines starting at the point and passing through the surface. [37] The concept can be extended to a solid body (such as a right circular cylinder) if that body can be decomposed into a set of limiting smooth parametric surfaces. Solid angles are usually measured in terms of the area subtended on a unit sphere centered on the point. Just as the length subtended by a curve on a unit circle centered on a point of interest gives the ordinary (2D) angle subtended in radians, the area subtended by a surface on a unit sphere centered on a point of interest gives the solid (3D) angle subtended in steradians.

[6]This solid angle calculation function is an implementation of the algorithm developed in reference [38].

Moderator (optional)

Detector (with glass shards)

Shield (optional)

Bounding Sphere

Source

Outer Source Sphere
(may be used for shielding)

Inner Source Sphere
(optional, may be used for shielding)
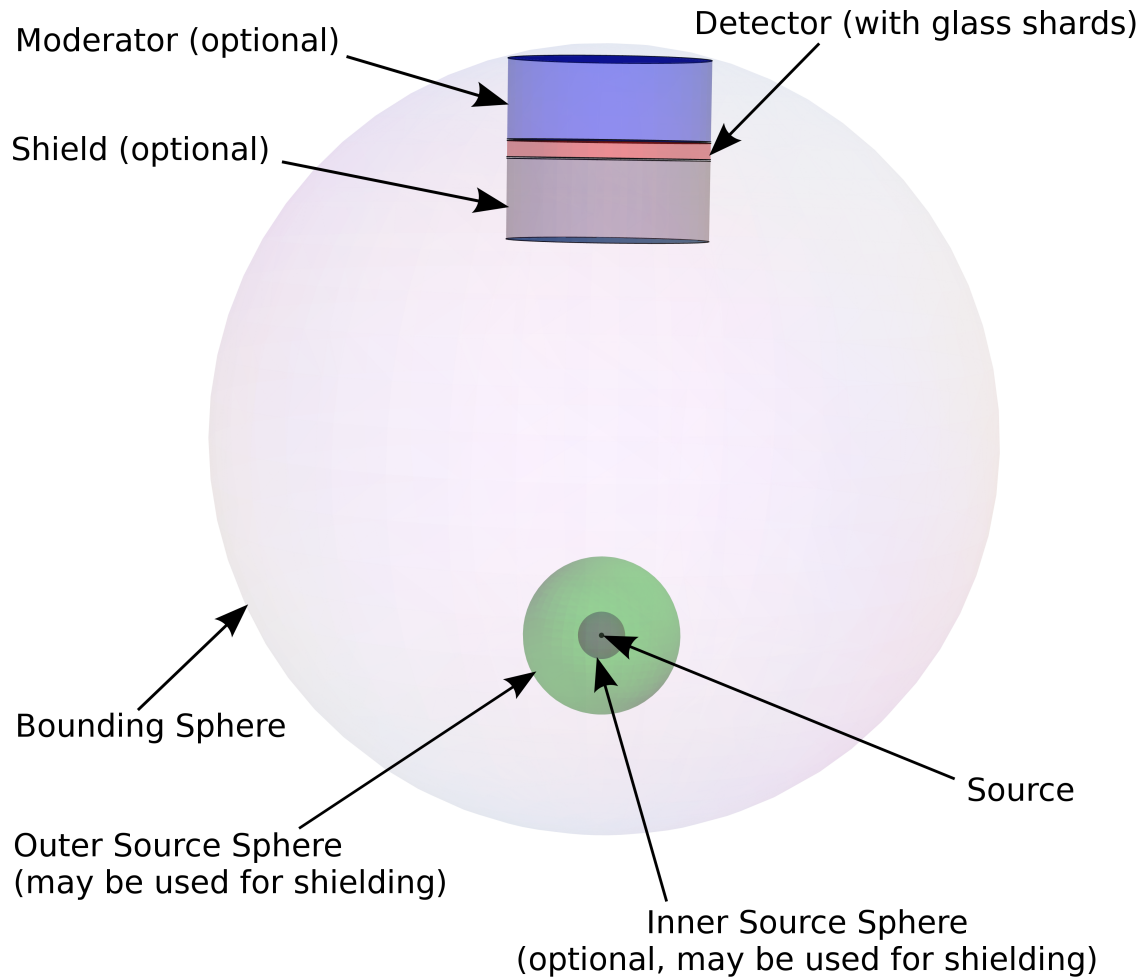
Figure 2.1 The package of Mathematica functions that I have developed allows the user to rapidly specify problem geometries such as the one shown here.

code package, please consult the online documentation (which, upon installation of the package, becomes accessible through Mathematica's built-in Documentation Center).

2.1.3 Simulation Calculations

The Monte Carlo simulations that I performed for this study generally focused on providing information about two quantities of interest: the neutron detection efficiency and gamma sensitivity of a given broken glass detector.

2.1.3.1 Neutron Detection Efficiency

To calculate the absolute neutron detection efficiency of a broken glass detector, I used MCNP to determine the probability that a neutron emitted by a ^{252}Cf point source would be captured by a ^{6}Li nucleus in one of the glass shards. I could then obtain the intrinsic neutron detection efficiency of the same detector by dividing this probability by the fractional solid angle (the solid angle in steradians divided by 4π) subtended by the detector at the source.[7]

Although this method for simulating the neutron detection efficiency of a ^{6}Li glass-based neutron detector has been used in the past and has agreed well with experiment (see, for example, reference [39]), the reader should be aware of two approximations that have been made. First, by calculating the theoretical efficiency in this manner, we assume that every neutron capture reaction leads to a corresponding bright scintillation pulse that is successfully registered by a photodetector and that exceeds the pulse height discrimination threshold in use. While this should not be far from the truth for a well-built neutron detector, certain factors (such as the leakage of neutron capture products out of the glass shards or comparatively poor light collection from certain regions of the detector) may cause the amplitude of a neutron scintillation pulse to dip below the pulse height

---

[7]Since the surface area of a unit sphere is 4π, the fractional solid angle subtended by a detector at an isotropic point radiation source in vacuum is equal to the probability that a particle emitted by the source will strike the detector.

discrimination threshold, while others (such as photodetector dead time or two neutron capture events that happen essentially simultaneously) may cause some neutron scintillation pulses to be overlooked entirely. Any systematic overestimates of the neutron detection efficiency of the simulated detectors due to these uncommon problems, however, are likely to be small compared with the statistical uncertainty present in the efficiency calculated by MCNP.[8]

Second, because the simulated intrinsic efficiencies are calculated by adjusting the absolute efficiencies based on the solid angle subtended by the detector at the source, any absorption of neutrons by shielding surrounding the source is not considered. Since the intrinsic neutron detection efficiency of a detector is defined as the fraction of neutrons striking the detector that are detected, our calculated intrinsic efficiencies will systematically underestimate the true intrinsic efficiencies whenever there is significant shielding around the source. However, because smuggled nuclear materials are likely to be well-shielded, this way of calculating the intrinsic efficiency of the detectors may be of more practical value and will be used whenever simulated intrinsic efficiencies are discussed in this paper.

2.1.3.2 Gamma Sensitivity

To determine the simulated gamma sensitivity of a broken glass detector, I used MCNP (or PENE-LOPE, when possible) to calculate a probability density histogram for energy deposition in one or more of the glass shards by a gamma ray emitted by a cobalt-60 (^{60}Co) point source. The histogram was always defined to have 100 equally spaced bins between 0 MeV and 1.4 MeV, and it was initially normalized so that integrating over its entire range would give the probability that a gamma ray emitted by the source would deposit a nonzero energy in one or more of the glass shards.

---

[8]I have recently become aware that it is possible to perform simulations using the related code package MCNPX that take alpha and triton leakage out of the glass into account. For more details, please see reference [40].

After obtaining this probability density histogram, I then renormalized it by dividing the value of each bin by the fractional solid angle subtended by the detector (an unshielded ^{60}Co source was always used). The simulated gamma sensitivity of the detector could then be obtained by integrating the renormalized probability density above an appropriate threshold. Because the simulated results were quite sensitive to this choice of threshold, a direct comparison with experiment was difficult. However, comparing the simulated gamma sensitivities of different detectors proved to be useful in guiding our design of prototype detectors and in understanding the physical processes occurring within them.

2.2 Simulation Results and Discussion

The Monte Carlo simulations that I conducted provide strong evidence that the gamma sensitivity of a broken glass detector is dramatically lower than a comparable detector constructed using a thin sheet of ^{6}Li glass, that the reason behind the lowered gamma sensitivity is a softer pulse height spectrum for the glass shards versus the glass sheet, and that the lowered gamma sensitivity can be maintained while achieving good neutron detection efficiency.

2.2.1 Average Energy Deposited by ^{60}Co Gammas in the Glass Shards

The broken glass detector is based on the theory that more electrons scattered by gamma rays will leak out of a group of small ^{6}Li glass shards than will leak out of a sheet of ^{6}Li glass of equal total volume. Based on this reasoning, I initially thought that the average energy deposited by a gamma ray in a group of the glass shards would be lower than the average energy it would deposit in a comparable glass sheet. However, simulations that I performed using PENELOPE demonstrated that this is not always the case.

To test my initial intuition, I conducted a series of PENELOPE simulations in which a small

cylindrical detector (~2.5 cm diameter, 7.72 cm thick) was bombarded with 1.33 MeV gamma rays[9] generated by an isotropic point source at a perpendicular distance of 1 m from the center of the front face of the detector. The detector consisted of a cylinder of PMMA with a 1 mm thick ^{6}Li glass sheet placed on top of it or 500 spherical ^{6}Li glass shards (each about 1 mm^3 in volume) embedded within it. Several versions of the broken glass detector were simulated. In each version, the glass shards were randomly dispersed within the PMMA cylinder, but the maximum allowed depth of a glass shard below the front face of the detector was varied between versions. Because the same total volumes of PMMA and ^{6}Li glass were used in all trials, the maximum glass depth served as a rough measure of how far the glass shards were separated from each other within the detector. For ease of comparison with the broken glass case, the detector constructed using a 1 mm thick glass sheet was assigned a glass depth of 1 mm.

The simulated average energies deposited in the ^{6}Li glass by gamma rays incident on each of the detectors mentioned above are shown in Fig. 2.2. Surprisingly, the average energy deposited by gamma rays in the glass sheet was significantly lower than the average energy deposited by gamma rays in the glass shards for all of the shard configurations tested. This result might be explained by considering the paths of electrons scattered by gamma rays in these detectors. Since all of the gamma rays that entered a detector in these simulations did so at approximately normal incidence, electrons scattered by these gamma rays will travel predominantly toward the back of the detector. Because the glass sheet is located in front of the entire PMMA cylinder, very few electrons scattered in the PMMA will enter the glass sheet. However, because most of the glass shards will be behind a significant thickness of PMMA, electrons scattered in the PMMA in front of the glass shards have a fair chance of entering the shards, increasing the average energy deposited within them.

This was a disappointing result because it seemed, at first glance, to suggest that the gamma

---

[9]This energy corresponds to the higher of two gamma ray energies emitted by ^{60}Co.

Average Energy Deposition in the ^{6}Li Glass per Incident γ
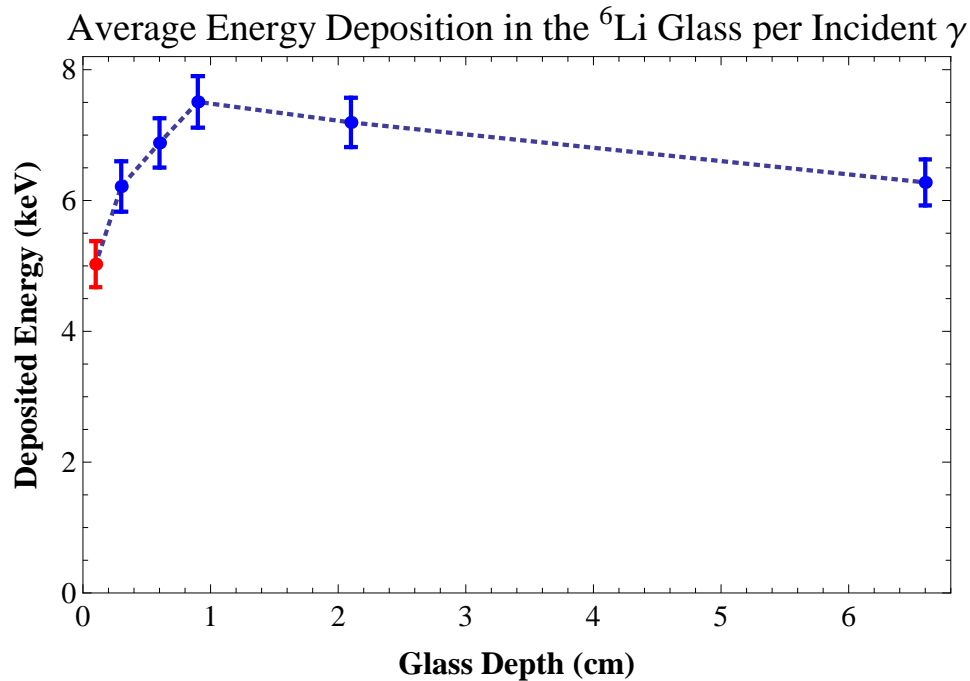
Red: Sheet of glass scintillator in front of a cylinder of poly(methyl methacrylate)

Blue: Glass spheres embedded within of a cylinder of poly(methyl methacrylate)

Figure 2.2 The simulated average energies deposited by 1.33 MeV gamma rays normally incident on a small ^{6}Li glass-based detector are shown above. The dashed blue line represents a linear interpolation between the data points and is included to show a general trend. The increasing average deposited energy for small glass depths is probably due to Compton electrons entering glass shards from the surrounding plastic.

sensitivity of a broken glass detector might be higher than that of a comparable glass sheet detector. However, careful analysis of simulated pulse height spectra for the two kinds of detector showed that, even when gamma rays deposit a higher average energy in glass shards than in a glass sheet, the gamma sensitivity of the glass shards will actually be significantly lower.

2.2.2 Pulse Height Spectrum Softening

Both MCNP and PENELOPE can simulate pulse height spectra (histograms describing the frequency or relative frequency of pulses produced in a detector as a function of their total energy or light output) by computing probability densities for energy deposition by source particles in a detector. To study the behavior of gamma rays and Compton electrons within the broken glass detector in more detail, I used PENELOPE to calculate this kind of probability density histogram for a variety of detectors constructed using ^{6}Li glass shards and sheets. Some typical results are shown in Fig. 2.3. Although the average deposited energy per incident gamma ray was usually greater in the glass shards than in comparable glass sheets, the probability of an incident gamma ray depositing a relatively high (~1 MeV or more) energy was consistently lower in the glass shards than in the glass sheets.

This result provided strong evidence that using shards of ^{6}Li glass to build a neutron detector instead of a thin sheet of glass could significantly reduce the gamma sensitivity of the system.

2.2.3 Neutron Detection Efficiency

In addition to investigating the gamma sensitivity of the broken glass detector using Monte Carlo methods, I performed simulations using MCNP to predict its neutron detection efficiency. One version of the broken glass detector that I studied extensively using these simulations was constructed using two disks of spherical ^{6}Li glass shards (each about 1 mm^3 in volume) embedded in a large cylinder (12.7 cm diameter, ~15 cm long) of PMMA (see Fig. 2.4). Each of the two disks of glass

Deposited Energy (MeV) vs. Probability Density (1/(MeV·particle))

Glass Sheet (1 mm thick) vs.

Glass Shards (dispersed in 4 mm thick region and scaled to equal total volume)
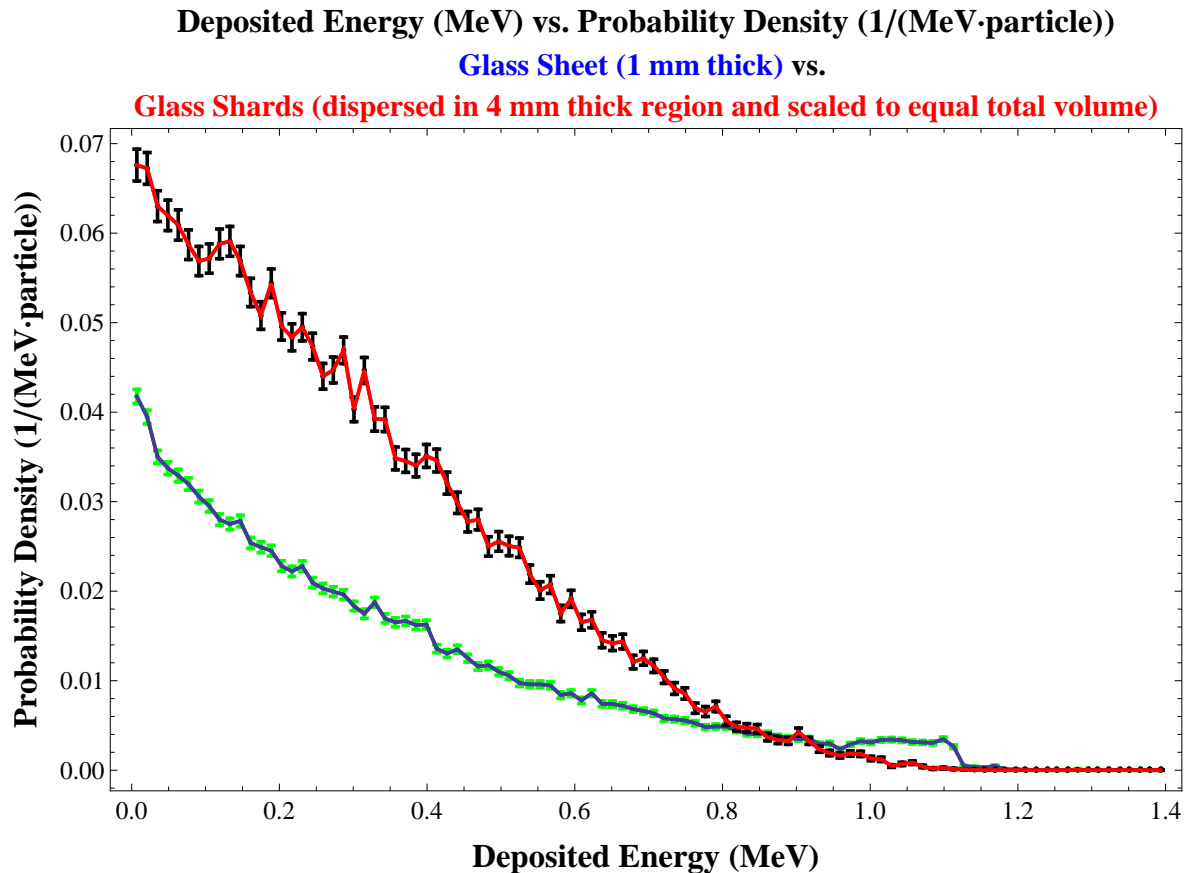
Figure 2.3 Simulated pulse height spectra for energy deposition by ^{60}Co gamma rays (both energies) normally incident on a detector constructed using a sheet of ^{6}Li glass scintillator (blue) and a broken glass detector (red) are shown above. Although the same amount of PMMA was used in each of these detectors, since the volumes of glass used were unequal, the glass shard results have been rescaled by an appropriate factor. Note that the spectrum for the glass shards is markedly softer in the region above about 1 MeV.

Figure 2.4 A depiction of the two-section broken glass detector is shown above. Rendering the many thousands of glass spheres positioned within the detector would be impractical, so only a few representative spheres are shown and the size of the detector is greatly reduced.

shards in this "two-section broken glass detector" had the same total volume of glass as a 1 mm thick sheet of glass with the same diameter as the detector. The glass shards in each disk were randomly positioned within a 3 mm thick region of the PMMA. One of the two disks was always placed just below the surface of the front face of the PMMA cylinder. The other was placed at various distances deeper inside the cylinder. A point ^{252}Cf source was placed directly in front of the detector at a distance of 1 m away, and various thicknesses of water were used to shield the source.

The calculated values of the intrinsic neutron detection efficiency for this detector as a function of disk separation (measured from the center of one disk to the center of the other) and the radius of a sphere of water surrounding the ^{252}Cf point source are shown in Fig. 2.5. The amount of shielding placed around the source strongly influenced the two section detector's intrinsic efficiency, boosting it from around 5% to around 25% as the radius of the water surrounding the source increased from 0 cm to 10 cm. The position of the second disk of glass shards had a comparatively weak effect on the detector's performance, but positioning it judiciously in situations with sparse source shielding still allows one to increase the efficiency of the detector by a few percent.
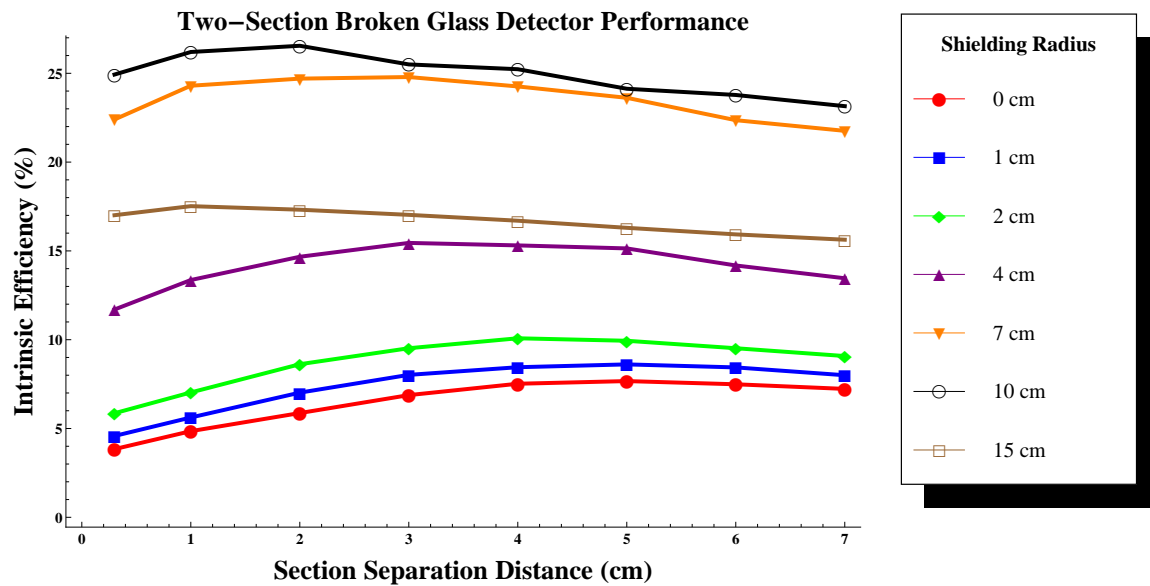
Figure 2.5 The intrinsic neutron detection efficiencies for various configurations of the two-section broken glass detector are shown above. Note that, as the source becomes more heavily shielded, the efficiency of this detector rapidly increases. The values for the intrinsic efficiency given here, as mentioned in section 2.1.3.1, do not take absorption of neutrons in the shielding around the source into account. As a result, the stated intrinsic efficiencies for the trials with very large amounts of shielding are substantially lower than the true values.

The results of this simulation strongly suggest that a form of the broken glass detector could achieve good to excellent neutron detection efficiency in a scenario similar to RPM testing conditions. Because smuggled nuclear materials are likely to be heavily shielded, a detector similar to the one simulated here could be particularly useful for homeland security applications.

2.3   Suggestions for Future Work

The simulations discusssed above represent only a small portion of the modeling of the broken glass detector that could be performed using Monte Carlo methods. Two simulations that could be performed in the future appear especially useful. First, a simulation of the neutron detection efficiency and gamma sensitivity of an array of broken glass detectors with roughly the same dimensions as a standard ^{3}He RPM neutron detector would be useful in assessing whether a large-scale version of the broken glass detector could serve as a ^{3}He replacement. Such a simulation could most easily be performed by using the Mathematica package described in this paper to define the geometry for one broken glass detector and then using an MCNP lattice to simulate many identical detectors arranged in a regular pattern. Second, future simulations could be used to find an optimal size for the ^{6}Li glass shards. One would probably need to use MCNPX to simulate the trajectories of the neutron capture products in the glass shards (using a method similar to the one presented in reference [40]) in order to avoid choosing a shard size for which triton leakage out of the glass is significant.

Chapter 3

Experimental Tests

To verify that the broken glass detector has a much lower gamma sensitivity than comparable detectors constructed using thin sheets of ^{6}Li-loaded glass scintillator, Dr. J. Bart Czirr and I tested several prototype broken glass detectors. We performed all of these experiments in the underground nuclear physics group laboratory at Brigham Young University. The detectors were always placed in a light-tight wooden box for testing. Signals from a photomultiplier tube (PMT) monitoring a detector being tested were passed through an amplifier and digitized using a 250 MHz CAEN digitizer. Data from the digitizer were collected using an acquisition program developed at BYU, and the digitized PMT pulse information was subsequently analyzed using a set of MATLAB routines. These MATLAB routines apply both pulse height and pulse shape discrimination to the digitized pulses using methods described in the second paragraph of section 1.3.3.4 and in reference [28].

I prepared shards of ^{6}Li glass scintillator for use in our experiments by crushing 1 mm thick sheets of the glass using a mortar and pestle. To ensure that all of the glass shards that we used were roughly the same size, I used two sieves to sort the crushed glass fragments. Shards that fell through a wire sieve with $2mm^2$ square holes but did not fall through a similar sieve with $1 mm^2$ holes were accepted for use in our experiments. Our decision to use this shard size was
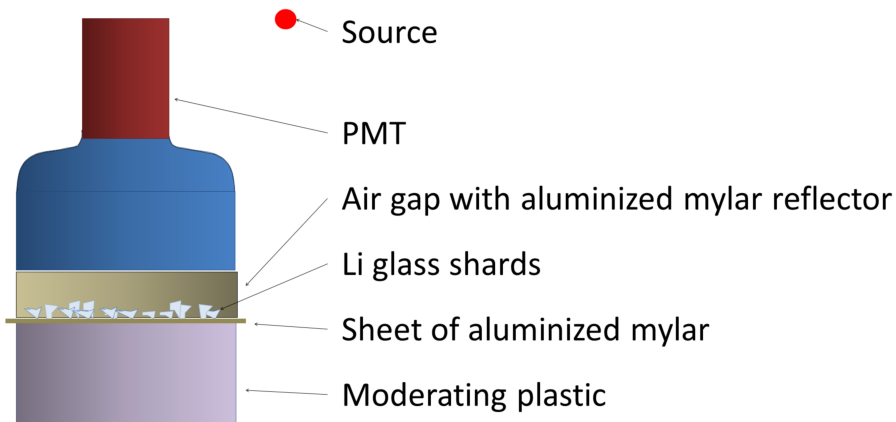
Figure 3.1 A diagram depicting the components of a very crude broken glass detector is shown above. This was the first broken glass detector that we tested.

based mainly on the size of the sieves that were readily available to us. Future work will probably determine that a different shard size is the optimal choice.

3.1 Initial Experiment

The first broken glass detector that we tested consisted of little more than some loose shards of ^{6}Li glass placed under a photomultiplier tube (see Fig. 3.1). To boost the efficiency of the glass shards, we placed a cylinder of plastic scintillator beneath them for moderation. The plastic scintillator was optically isolated from the glass shards (so that only light from the glass would reach the PMT) by a layer of aluminized mylar. A tube of aluminized mylar was also placed around the glass shards to reflect as much light as possible into the PMT.

To measure the gamma sensitivity of the detector described above, we first exposed the detector to a ^{252}Cf neutron source so that appropriate pulse area and pulse shape discrimination thresholds could be set. Once this was done, we measured the background neutron detection rate by allowing the detector to run for several hours without any source present. We then irradiated the detector with a ^{60}Co source so that 4.2×10^6 gamma rays were incident on the detector. By subtracting

the number of expected background neutron events from the number of "neutron" detections registered by the detector in the presence of the ^{60}Co source, we determined that this simple detector misidentified only -5 ± 8 of the 4.2×10^6 incident gamma rays as neutrons.[1]

This result was very encouraging because the measured gamma sensitivity of the detector was lower than the DHS requirement of 10^{-6} for all RPM neutron detectors.

3.2 A Permanent Broken Glass Detector

Although our makeshift broken glass detector functioned remarkably well, constructing a permanent version would be necessary. Over the course of several months, we tried embedding shards of ^{6}Li glass in a wide variety of transparent materials. The first material that we used was sodium silicate. Although the optical clarity of this material was good enough that I built several detectors using it, we quickly found that it warps, cracks, and becomes cloudy over the course of several days when it is exposed to air. We tried embedding the glass shards in a variety of other materials, including silicone oil, EPO-TEK optical epoxy, clear glue, nail polish, and varnish, but all of these materials transmitted the light from the glass shards very poorly. During our search for a suitable matrix in which to embed the glass shards, PMMA appeared to be a good option for a long time. However, getting methyl methacrylate (the monomer that forms PMMA) to polymerize correctly (i.e., with an approximately uniform index of refraction) around the glass shards proved to be very difficult for some unknown reason.

Our best current broken glass detector (see Fig. 3.2) is constructed by placing shards of ^{6}Li glass in a Pyrex petri dish, pouring a thin (~1 mm thick) layer of Eljen EJ-500 optical epoxy over them, and then adjusting the positions of the glass shards so that they are as far away from one

---

[1]The result reported here is negative because the number of events identified as neutrons by the detector was smaller than the number of neutron detections we would expect based on our previous measurement of the level of background neutron radiation in the lab.
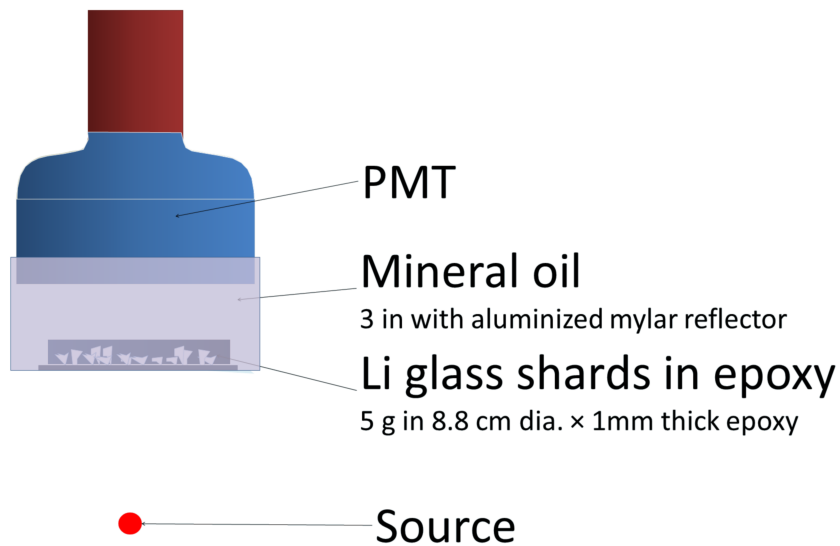
Figure 3.2 The permanent broken glass detector design that we are currently using in our experiments is shown above. Our early prototypes have used petri dishes that have a diameter of 8.8 cm, but a larger version using a petri dish with approximately the same diameter as the phototube could easily be made.

another as possible. After the epoxy has hardened, the petri dish is submerged in 3 inches of mineral oil for moderation and for good optical coupling to a PMT.

We measured the gamma sensitivity of this detector by irradiating it two separate times using a ^{252}Cf source and a ^{60}Co source. In both trials, each pulse from the photomultiplier tube was digitized and integrated. A graph of the pulses obtained from the PMT in both of these trials is shown in Fig. 3.3.

Using the pulse information recorded in the presence of the ^{252}Cf, we were able to define a "neutron window" in which the vast majority of the pulses generated by neutrons would be found. This window consists of an upper and lower limit on a pulse's total area (a form of pulse height discrimination) and similar limits on the fraction of a pulse's total area that occurred before a given elapsed time[2] (a form of pulse shape discrimination). While the choice of these limits is not

---

[2]The elapsed time for the PMT pulses is measured from the time that the pulse first crossed the digitizer's trigger threshold.
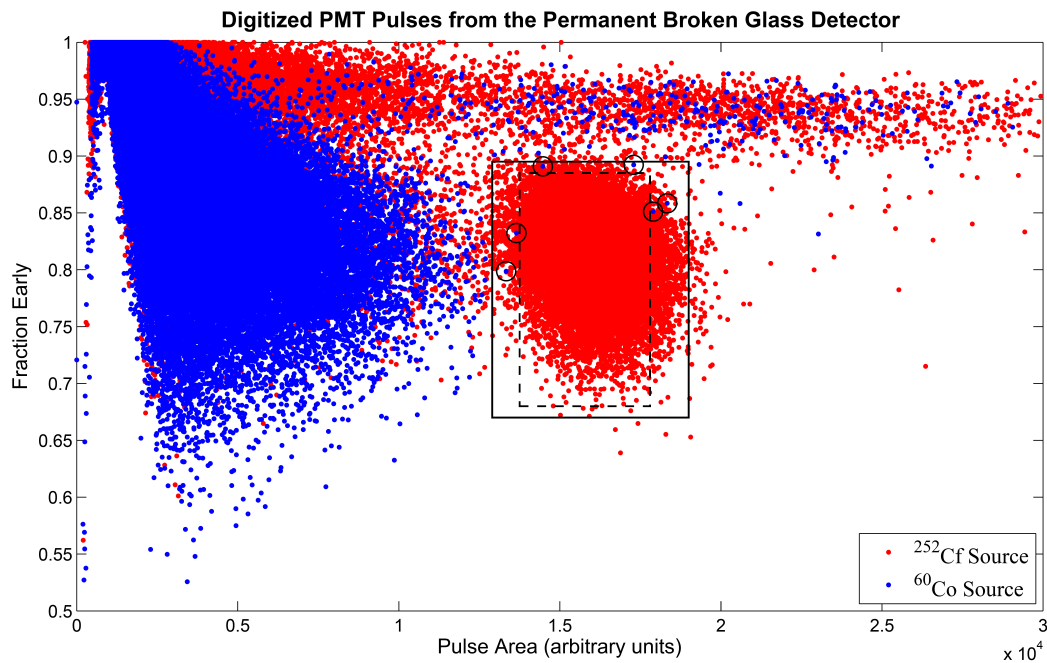
Figure 3.3 This graph displays information about the digitized PMT pulses recorded with our permanent broken glass detector in the presence of a ^{252}Cf source (red) and a ^{60}Co source (blue). The horizontal axis measures the total integrated area of the pulses, while the vertical axis measures the fraction of this area that occurs before a certain elapsed time. Depending on the choice of neutron window, the measured gamma sensitivity ranged between about 8×10^{-7} (solid box) and zero (dashed box). Gamma ray pulses that were found in the larger neutron window are circled.

arbitrary (choosing a window that is too big will cause the detector to misidentify pulses originating from a variety of other processes as neutron capture pulses), an experimenter has a fair amount of flexibility in choosing their exact values. In particular, if one is willing to slightly reduce the neutron detection efficiency of a detector, one can often significantly reduce its gamma sensitivity by shrinking the size of the neutron window. Two reasonable choices of neutron window for our permanent broken glass detector are shown as boxes in Fig. 3.3.

After identifying our pulse height and pulse shape discrimination thresholds using a ^{252}Cf source, we irradiated our permanent broken glass detector with ^{60}Co gamma rays. During the experiment, 8×10^6 of these gamma rays were incident on the Pyrex petri dish holding the glass shards. For our larger choice of neutron window (the solid box in Fig. 3.3), 6 of these gamma rays were misidentified by the detector as neutrons, giving the detector a measured gamma sensitivity of about 8×10^{-7}, which is just below the DHS requirement. If we are willing to make a small sacrifice in efficiency to ensure that the gamma sensitivity of the broken glass detector is considerably lower than this, we can use the smaller neutron window (the dashed box in Fig. 3.3). This window still contains approximately 92% of the neutron pulses surrounded by the larger window, but none of the gamma ray pulses are located inside it. Therefore, if this window is used, the detector will have a gamma sensitivity of approximately zero.

Previous work by my research group showed that, using similar methods, the gamma sensitivity of a detector constructed using a 1 mm thick sheet of ^{6}Li glass could only be reduced to about 10^{-4} without significantly reducing the detector's neutron detection efficiency. [28] The broken glass detector therefore achieves a gamma sensitivity that is at least 100 times lower than comparable glass sheet detectors.

3.3   Conclusions and Suggestions for Future Work

In this thesis, I have presented a new technique for reducing the gamma sensitivity of a neutron detector constructed using ^{6}Li glass scintillator. Evidence from both Monte Carlo simulations and experiments shows that a broken glass detector will have a much lower gamma sensitivity than a comparable detector constructed using a thin sheet of ^{6}Li glass. Results from MCNP simulations also indicate that a broken glass detector can achieve good neutron detection efficiency, especially for sources that are heavily shielded.

The results I have presented here suggest that the broken glass detector might be useful as a possible replacement for ^{3}He-based neutron detectors for homeland security applications. However, much experimental work remains to be done. A full evaluation of the broken glass detector's potential as an RPM component can only be completed if an array of broken glass detectors can be built and tested. First steps toward that goal might involve building and testing a broken glass detector that contains a disk of glass shards and epoxy with the same diameter as the front face of a standard photomultiplier tube. To ensure that an array of broken glass detectors would have the same efficiency as a ^{3}He tube, it is likely that placing several disks of glass shards in each detector will be necessary. Future research could therefore focus on building and characterizing a broken glass detector composed of several such layers suspended in mineral oil. Because the low gamma sensitivity of this detector might also make it attractive for low-energy neutron time-of-flight measurements, searching for a transparent, non-hydrogenous material to cover the glass pieces would probably also be worthwhile. If a large-scale version of the broken glass detector can maintain low gamma sensitivity and high neutron detection efficiency, it could prove to be a valuable tool for studying neutron physics and preventing nuclear terrorism.

Appendix A

Photon Interactions with Matter

Photons, or quanta of light, interact with other particles in a wide variety of ways via the electromagnetic force. However, when we consider the possible interactions of relatively low-energy (~0.01 MeV–10 MeV) gamma ray photons with atoms, only three processes are generally important: photoelectric absorption, Compton scattering, and pair production. [41]

A.1   Photoelectric Absorption

Photoelectric absorption occurs when a photon is completely absorbed by an electron in an atomic electron cloud. Although photons often scatter off of free electrons, it can easily be shown[1] that the

---

[1]Although photoelectric absorption is an inherently quantum-mechanical process, one can establish that it is impossible for a free electron to completely absorb an incident photon using only elementary special relativity. Choose a reference frame in which a free electron is initially at rest and a photon is approaching it from an arbitrary direction. Before the photon is close to the electron, the electron has momentum $p_{e,i} = 0$ and energy $E_{e,i} = m_e c^2$, where m_e is the rest mass of the electron. The photon has frequency ν, energy $E_\gamma = h\nu$, and momentum $p_\gamma = \frac{h\nu}{c}$. Now suppose that the photon is completely absorbed by the electron. By conservation of energy, we see that the energy of the electron after the photoelectric absorption event must be $E_{e,f} = h\nu + m_e c^2$. Conservation of momentum tells us that the momentum of the electron after the absorption must be $p_{e,f} = \frac{h\nu}{c}$. From the definitions of momentum and energy in special relativ-

37

laws of conservation of energy and momentum preclude the possibility of photoelectric absorption by unbound electrons. After a photon is fully absorbed by an atomic electron, the electron is ejected from the atom with a kinetic energy given by the relation

$$T = h\nu - E_b$$

where h is Planck's constant, ν is the frequency of the absorbed photon, and E_b is the binding energy of the atomic electron. [41] The total photoelectric absorption cross section[2] per atom σ_A is approximately proportional to

$$\frac{Z^n}{E^{7/2}}$$

where the incident photon has an energy E between about 0.1 MeV and 10 MeV, the atom has atomic number Z, and the parameter n varies between 4 and 5 as a function of gamma ray energy. [19,41]

---

ity, it follows that these two quantities are related via the Pythagorean relation $E_{e,f} = \sqrt{\left(p_{e,f}c\right)^2 + \left(m_ec^2\right)^2}$. Inserting the values found previously for $E_{e,f}$ and $p_{e,f}$ into this equation, we find that $h\nu + m_ec^2 = \sqrt{(h\nu)^2 + (m_ec^2)^2}$. This implies that $\left(h\nu + m_ec^2\right)^2 = (h\nu)^2 + 2(h\nu)\left(m_ec^2\right) + \left(m_ec^2\right)^2 = (h\nu)^2 + \left(m_ec^2\right)^2$, so $2(h\nu)\left(m_ec^2\right) = 0$, and therefore either $E_\gamma = h\nu = 0$ or $m_e = 0$. Since both of these quantities are nonzero, it follows from the resulting contradiction that photoelectric absorption cannot occur for a free electron.

[2]The cross section σ for an interaction is proportional to the probability of that interaction occuring. Specifically, for a given flux of projectiles $n_{inc} = \frac{N_{inc}}{A}$ through a region of interest with cross-sectional area A, the cross section σ for a given reaction is defined as $\sigma \equiv \frac{N}{n_{inc}}$, where N is the total number of instances of the reaction that occur after N_{inc} projectiles have entered the region. [42] The relative frequency of the reaction (the average number of reactions per incident projectile) is therefore $\frac{N}{N_{inc}}$. Probability theory postulates that the relative frequency of an event will approach the true probability as the number of trials approaches infinity, so the probability P_{react} of an incident projectile undergoing the reaction is therefore given by $P_{\text{react}} = \lim_{N_{inc} \to \infty} \frac{N}{N_{inc}} = \lim_{N_{inc} \to \infty} \frac{N}{A\, n_{inc}} = \lim_{N_{inc} \to \infty} \frac{\sigma}{A}$. [43]

A.2   Compton Scattering

Compton scattering occurs when a photon collides with an electron (the electron may be bound or unbound) and transfers some of its energy to the electron. As a result of this transfer of energy, the photon's frequency decreases and it is deflected in a new direction. Using basic relativistic kinematics, the relationship between the change in the wavelength $\Delta\lambda$ of the scattered photon (the wavelength is related to the frequency by $\lambda = \frac{c}{\nu}$) and the angle between the photon's incident and scattered directions θ can be shown to be (see reference [42] for a typical argument)

$$\Delta\lambda = \lambda - \lambda_0 = \frac{h}{m_e c}\left(1 - \cos\left(\theta\right)\right).$$

A detailed theoretical treatment of the total cross section for Compton scattering is beyond the present scope but available elsewhere. [41] The total Compton scattering cross section per atom σ_C is approximately proportional to

$$\frac{Z}{\sqrt{E}}$$

where Z is the atomic number of the atom and E is the initial energy of the photon. [44]

A.3   Pair Production

Pair production is an interaction between a photon and the electric field of an atom in which the photon is completely absorbed and then replaced by an electron-positron pair. The electron-positron pair has a total energy equal to the energy of the absorbed photon. [41] This interaction can only occur when the incident photon has an energy greater than two times the rest energy of an electron ($2m_e c^2 \approx 1.022$ MeV). The positron will eventually annihilate with an electron from its surroundings, creating two new gamma rays that may subsequently interact with the surrounding matter. [19] The total pair production cross section per atom σ_P is approximately proportional to

$$Z^2 \ln\left(\frac{2E}{m_e c^2}\right)$$

for all values of the incident gamma ray energy $E \geq m_e c^2$. [44]

Appendix B

Scintillation Mechanism of ^{6}Li-loaded Glass Scintillator

Like other solid-state inorganic scintillators, ^{6}Li-loaded glass scintillator produces light as a result of processes dependent upon its electronic band structure. In crystalline solids, atoms are arranged in a nearly regular three-dimensional lattice. Rare irregularities in the lattice are due to the presence of defects and impurities in the crystal, which often exert a strong influence on the crystal's electrical and mechanical properties. [45] If we ignore the finite size of a crystal,[1] regard its atomic nuclei as essentially stationary, neglect irregularities in its structure, and omit interactions between its electrons, then the potential energy of an electron in the crystal as a function of position will be periodic. It can be shown[2] that the allowed energies for electrons in a periodic potential will form bands that are approximately continuous and that are separated by forbidden regions called gaps.

---

[1] Although all real solids have surfaces, the influence of surface effects on electronic structure can generally be considered a negligible perturbation. This is because the ratio of the number of atoms that form the surface of a solid to the number of atoms inside the solid is typically on the order of 10^{-8}. [45]

[2] See reference [45] for a three-dimensional derivation and reference [46] for a simplified but insightful derivation for a one-dimensional lattice.

The two most important energy bands in a crystal are the valence band and the conduction band. The valence band of a crystal is the highest range of energies that is normally occupied by electrons at absolute zero temperature. Electrons with energies in or below the valence band are bound to atoms in the lattice. The conduction band is the first energy band above the valence band. Electrons with energies in this band and above are free to move within the atomic lattice. The forbidden region between the upper end of the valence band and the lower end of the conduction band is known as the band gap. [47] Although glasses are amorphous materials (they lack the long-range order found in crystals), they also possess band gaps due to certain regularities in their atomic structure.[3]

When a charged particle or photon interacts via the electromagnetic force with an electron in the valence band of a solid, the electron may gain enough energy to cross the band gap and enter the conduction band. The electron will then move through the solid and may eventually de-excite back to the valence band by emitting a photon to carry off the excess energy. Although this simple process may produce many photons within a solid, it is unattractive for use in scintillators for several reasons. First, although electrons can spontaneously return to the valence band from the conduction band, they generally take a long time to de-excite across the band gap. [50] Second, the band gap is usually large enough that a photon emitted when a conduction-band electron fell to the valence band would have too much energy to be near the visible range. Since typical light detectors (e.g., photomultiplier tubes) are most sensitive to wavelengths in the visible and near-ultraviolet ranges, scintillators that produce visible light are desirable. Third, since the energy of

---

[3]The band gap found in glasses arises because the arrangement of atoms within them may be described by a regular graph. In graph theory, a graph is a collection of objects, referred to as vertices or nodes, that are linked in pairs via edges. A regular graph is a graph in which every vertex has the same number of edges. For covalent glasses such as window glass or ^{6}Li-loaded glass scintillator, molecules and the covalent bonds between them may be realistically modeled as the vertices and edges of a regular graph. [48] The existence of a band gap in glass has been shown to be a result of the regularity of this graph. [49]

the photons emitted by the de-excitation of electrons to the valence band from the conduction band is approximately the same as the energy required to promote a valence electron to the conduction band, valence electrons in the solid are likely to absorb much of the scintillation light. [19]

To avoid these problems and produce efficient scintillators, manufacturers often alter the typical conduction electron de-excitation process by adding activators, or specially chosen impurities, to the atomic lattice of a scintillator. In the case of ^{6}Li-loaded glass scintillator, the activator is Ce^{3+}, a form of the element cerium that has three fewer electrons than usual.[4] Activators are chosen so that their presence within the solid allows some of the electrons around them to occupy energy levels within the normally forbidden band gap. If a conduction electron enters one of the excited states created by the activator and then decays to the activator ground state, it can emit a photon with less energy than photons emitted by conduction electron decays to the valence band. If the activator is appropriately chosen, this photon will have a wavelength in a range suitable for efficient detection by a photodetector. [51] Since this photon will have significantly less energy than is required to promote valence electrons to the conduction band, it will generally be able to escape the scintillator without being absorbed. [19]

In order for a conduction electron to be able to enter an excited activator state and de-excite to the ground state, there must be a vacancy for it to fill in the outer part of the electron cloud of an activator atom. In the case of Ce^{3+}, since there is only one outer electron (in the 4f orbital), this electron must be removed before useful scintillation by a conduction electron can take place. Although this electron can be removed from its orbital in a variety of ways (e.g., via the photoelectric effect, Compton scattering, or a collision with a charged particle), it will usually be removed by an electron hole[5] that has migrated to the activator from somewhere else in the glass. Electron holes

---

[4]The electron configuration of unionized cerium is $1s^2 2s^2 2p^6 3s^2 3p^6 4s^2 3d^{10} 4p^6 5s^2 4d^{10} 5p^6 6s^2 5d^1 4f^1$. Cerium(III) has its three outermost electrons ($6s^2 5d^1$) removed, leaving a single outer electron in the 4f orbital.

[5]Electron holes are fictional entities that are used to represent the absence of an electron in an energy level in the valence band. [45] Whenever a valence electron is promoted to the conduction band, a hole is formed in the orbital that

are formed whenever valence electrons are raised to the conduction band anywhere in the glass, and they are free to move between valence electron orbitals. However, because the ionization energy of the Ce^{3+} activator atoms is less than that of the other atoms in the glass (i.e., less energy is required to remove the outer electron of Ce^{3+} than is required to promote a valence electron to the conduction band), electron holes tend to become trapped in the 4f orbital of the Ce^{3+} atoms. [19] When a conduction electron enters the vicinity of a Ce^{4+} ion (a Ce^{3+} ion with a trapped hole), it may drop into an excited state in the ion's electron cloud (typically the 5d state) and then de-excite further to recombine with the hole and re-occupy the 4f orbital. [52] This electron will usually emit a photon with a wavelength of about 395 nm.[6] A charged particle traveling through the glass (e.g., an alpha particle or triton created by a neutron capture reaction in a ^{6}Li nucleus) will create many electron-hole pairs. Some of these electron-hole pairs will migrate to the vicinity of Ce^{3+} ions in the glass and radiatively recombine, producing many scintillation photons. The resulting pulses of light are used to create electrical pulses in a photodetector that indicate that neutrons are being captured in the glass.

---

it previously occupied. Another valence electron can now occupy the empty orbital, but in doing so its original orbital is vacated. We can describe this event from a different but equivalent perspective by saying that the hole has moved. Although the difference in this case is trivial, when a long chain of orbital evacuations followed by orbital occupations occurs, it is much easier to describe the process in terms of a single moving hole than many moving electrons. By tracking the location of electron holes instead of valence electrons in the valence band, our description of phenomena in the valence band can be greatly simplified.

[6]Because the 5d orbital is on the surface of the Ce^{3+} ion, its energy level is strongly influenced by the electromagnetic field of the surrounding atoms in the glass. Since the glass's atomic arrangements do not show any long-range pattern, this field varies with position and results in a band of energies for photons being emitted as a result of 5d→4f transitions in the Ce^{3+} ions. This band is centered at a wavelength of 395 nm. [24]

Bibliography

[1] J. Medalia, ""Dirty Bombs": Technical Background, Attack Prevention and Response, Issues for Congress," Technical report, Congressional Research Service, Washington, DC (2011) .

[2] J. Ely, "Radiation Detection for Homeland Security: Past, Present, and Future,", 2006, presentation Given at the 2006 Annual Meeting of the Health Physics Society.

[3] National Nuclear Security Administration, "Fact Sheet: NNSA's Second Line of Defense Program,", 2011.

[4] S. P. Clarke, "Radiation Detection, Response & Recovery,", PowerPoint Presentation given at the International Conference on Control and Management of Radioactive Material Inadvertently Incorporated into Scrap Metal, 23-27 February 2009, Tarragona, Spain, 2009.

[5] National Nuclear Security Administration, "Megaports Initiative," (2010).

[6] R. T. Kouzes, "Detecting Illicit Nuclear Materials," American Scientist **93,** 422–427 (2005).

[7] R. T. Kouzes, E. R. Siciliano, J. H. Ely, P. E. Keller, and R. J. McConn, "Passive neutron detection for interdiction of nuclear material at borders," Nuclear Instruments and Methods in Physics Research Section A: Accelerators, Spectrometers, Detectors and Associated Equipment **584,** 383–400 (2008).

[8] R. V. Ginhoven, R. Kouzes, and D. Stephens, "Alternative Neutron Detector Technologies for Homeland Security," Technical Report No. PNNL-18471, Pacific Northwest National Laboratory, Richland, Washington (2009) .

[9] Government Accountability Office, "Technology Assessment: Neutron Detectors: Alternatives to using helium-3,", 2011.

[10] R. T. Kouzes, "The ^{3}He Supply Problem," Technical Report No. PNNL-18388, Pacific Northwest National Laboratory, Richland, Washington (2009) .

[11] J. H. Ely, L. E. Erikson, R. T. Kouzes, A. T. Lintereur, and D. C. Stromswold, "Lithium Loaded Glass Fiber Neutron Detector Tests," Technical Report No. PNNL-18988, Pacific Northwest National Laboratory (2009) .

[12] Kouzes, J. Ely, A. Lintereur, E. Siciliano, and M. Woodring, "BF3 Neutron Detector Tests,", 2009.

[13] R. T. Kouzes, J. H. Ely, L. E. Erikson, W. J. Kernan, D. C. Stromswold, and M. L. Woodring, "Full Scale Coated Fiber Neutron Detector Measurements," Technical Report No. PNNL-19264, Pacific Northwest National Laboratory, Richland, Washington (2010) .

[14] A. T. Lintereur, R. T. Kouzes, J. H. Ely, L. E. Erikson, and E. R. Siciliano, "Boron-Lined Neutron Detector Measurements," Technical Report No. PNNL-18938, Pacific Northwest National Laboratory, Richland, Washington (2009) .

[15] R. Kouzes and J. Ely, "Status Summary of ^{3}He and Neutron Detection Alternatives for Homeland Security,", 2010.

[16] R. C. Runkle, A. Bernstein, and P. E. Vanier, "Securing special nuclear material: Recent advances in neutron detection and their role in nonproliferation," Journal of Applied Physics **108,** 111101 (2010), m3: Article.

[17] Domestic Nuclear Detection Office, "Functional Requirements Document (FRD) For Radiation Portal Monitor Systems (RPMS) ^{3}He Neutron Detection Module (NDM) Replacement,", 2010, 600-NDRP-113410v2.07.

[18] R. T. Kouzes, J. R. Ely, A. T. Lintereur, and D. L. Stephens, "Neutron Detector Gamma Insensitivity Criteria," Technical Report No. PNNL-18903, Pacific Northwest National Laboratory, Richland, Washington (2009) .

[19] G. F. Knoll, *Radiation Detection and Measurement*, 4th ed. (Wiley, 2010).

[20] R. C. Martin, J. B. Knauer, and P. A. Balo, "Production, distribution and applications of californium-252 neutron sources," Applied Radiation and Isotopes **53,** 785–792 (2000).

[21] J. Ely, R. Kouzes, J. Schweppe, E. Siciliano, D. Strachan, and D. Weier, "The use of energy windowing to discriminate SNM from NORM in radiation portal monitors," Nuclear Instruments and Methods in Physics Research Section A: Accelerators, Spectrometers, Detectors and Associated Equipment **560,** 373–387 (2006).

[22] R. T. Kouzes and E. R. Siciliano, "The response of radiation portal monitors to medical radionuclides at border crossings," Radiation Measurements **41,** 499–512 (2006).

[23] Saint Gobain Crystals, "Glass Scintillator Data Sheet,", 2007.

[24] A. R. Spowart, "Neutron Scintillating Glasses: Part 1: Activation by external charged particles and thermal neutrons," Nuclear Instruments and Methods **135,** 441–453 (1976).

[25] L. M. Bollinger and G. E. Thomas, "Measurement of the Time Dependence of Scintillation Intensity by a Delayed Coincidence Method," Review of Scientific Instruments **32,** 1044–1050 (1961).

[26] C. Coceva, "Pulse-shape Discrimination with a Glass Scintillator," Nuclear Instruments and Methods **21,** 93–96 (1963).

[27] R. A. Winyard, J. E. Lutkin, and G. W. McBeth, "Pulse Shape Discrimination in Inorganic and Organic Scintillators I," Nuclear Instruments and Methods **95,** 141–153 (1971).

[28] A. A. Wallace, Bachelor thesis, Brigham Young University, 2011.

[29] F. D. Brooks, "General Survey on Choice of the Detector for a Time-of-Flight Experiment," In *Neutron time-of-flight methods: proceedings of a symposium organized by European-American Nuclear Data Committee in collaboration with Centre d'études nucleaires de Saclay (France) and Institut national des sciences et techniques nucleaires, Saclay, 24-27 July, 1961*, J. Spaepen, ed., pp. 389–405 (European Atomic Energy Community (Euratom), 1961).

[30] G. L. Jensen and J. B. Czirr, "Gamma-ray sensitivity of ^{6}Li-glass Scintillators," Nuclear Instruments and Methods **205,** 461–463 (1983).

[31] T. Matsumoto, H. Harano, T. Shimoyama, A. Uritani, Y. Sakurai, and K. Kudo, "Development of a novel small-sized neutron detector based on a 6Li-glass scintillator," In *Nuclear Science Symposium Conference Record, 2005 IEEE*, **3,** 1291 – 1293 (2005).

[32] T. Matsumoto, H. Harano, A. Masuda, J. Nishiyama, Y. Sakurai, and A. Uritani, "New idea of a small-sized neutron detector with a plastic fibre," Radiation Protection Dosimetry **146,** 92–95 (2011).

[33] A. R. Spowart, "Measurement of the Gamma Sensitivity of Granular and Glass Neutron Scintillators and Films," Nuclear Instruments and Methods **82,** 1–6 (1970).

[34] R. W. Perkins, P. L. Reeder, N. A. Wogman, R. A. Warner, D. W. Brite, W. C. Richey, and D. S. Goldman, "Method and Apparatus for Detecting Neutrons,", 1997.

[35] X-5 Monte Carlo Team, "MCNP: A General Monte Carlo N-Particle Transport Code, Version 5,", 2003.

[36] F. Salvat, J. M. Fernández-Varea, and J. Sempau, *PENELOPE-2008: A Code System for Monte Carlo Simulation of Electron and Photon Transport*, Facultat de Física (ECM), Universitat de Barcelona, Spain, 2008.

[37] J. Stewart, *Multivariable Calculus: Early Trancendentals*, 6th ed. (Thomson Brooks/Cole, McMaster University, 2008), p. 1109.

[38] M. J. Prata, "Solid angle subtended by a cylindrical detector at a point source in terms of elliptic integrals," Radiation Physics and Chemistry **67,** 599–603 (2003).

[39] J.-C. Wang, Ph.D. thesis, Brigham Young University, 1991.

[40] M. R. Williamson, Ph.D. thesis, University of Tennessee - Knoxville, 2010.

[41] R. D. Evans, *The Atomic Nucleus* (Tata McGraw Hill, 1955).

[42] J. R. Taylor, C. D. Zafiratos, and M. A. Dubson, *Modern Physics for Scientists and Engineers*, 2nd ed. (Pearson Prentice Hall, 2004).

[43] R. Epstein, *The Theory of Gambling and Statistical Logic* (Academic Press, 2009).

[44] M. D. Birowosuto, Ph.D. thesis, Technical University of Delft, 2007.

[45] E. Kaxiras, *Atomic and Electronic Structure of Solids* (Cambridge University Press, 2003).

[46] D. J. Griffiths, *Introduction to Quantum Mechanics*, 2nd ed. (Pearson Prentice Hall, 2005).

[47] C. Kittel, *Introduction to Solid State Physics*, 7th ed. (John Wiley and Sons, Inc., 1996).

[48] J. J. Meghirditchian, "Study of the Relationship between Specific Volume and Composition for Me20-Si02 and MeF-BeF2 Glasses with a Random Graph Model," Journal of the American Chemical Society **113,** 395–397 (1991).

[49] N. Rivier, "Continuous random networks: From graphs to glasses," Advances in Physics **36,** 95–134 (1987).

[50] E. Yablonovitch, "The chemistry of solid-state electronics," Science **246,** 347–51 (1989).

[51] F. A. Smith, *A Primer in Applied Radiation Physics* (World Scientific, 2000).

[52] S. Shionoya, "Photoluminescence," In *Luminescence of Solids*, D. R. Vij, ed., pp. 95–133 (Plenum Press, 1998).